

---

**MHD Mixed Convection Stagnation-Point Flow of a Power - Law Nano fluid towards a Stretching Surface in the presence of viscous dissipation and suction or injection**

**1 K.Padmavathi , Lecturer in Mathematics P.A.S.College Pedanandipadu**

**2 Y.Anitha kumari , Lecturer in Mathematics J.K.C. College Guntur**

**ABSTRACT**

Two-dimensional MHD mixed convection boundary layer flow of heat and mass transfer stagnation-point flow of a non-Newtonian power-law Nano fluid towards a stretching surface with thermal radiation and heat source/sink in the presence of viscous dissipation and variable suction/injection is investigated numerically. "The governing partial differential equations are converted into nonlinear, ordinary, and coupled differential equations and are solved using bvp4c Matlab solver. The numerical results are compared with the published data and are found to be in good agreement

**.Keywords:** MHD, Mixed convection, Heat and Mass Transfer, Viscous Dissipation, Heat Source/Sink, Suction/injection.

**INTRODUCTION**

Many of the non-Newtonian fluids encountered in chemical engineering processes are known to follow the empirical Ostwald-de Waele power-law model. The concept of boundary layer was applied to power-law fluids by Schowalter [1]. Hatami et al. [2] studied the heat transfer and flow analysis for a non-Newtonian third grade nanofluid flow in porous medium of a hollow vessel in the presence of magnetic field. Rashad et al. [3] studied the effect of uniform transpiration velocity on free convection boundary-layer flow of a non-Newtonian fluid over a permeable vertical cone embedded in a porous medium saturated with a nanofluid. Keshavarz Moraveji and Beheshti [4] investigated the forced convection heat transfer of non-Newtonian nanofluids in a horizontal tube with constant wall temperature under turbulent flow conditions using computational fluid dynamics tools. Khan et al. [5] investigated the non-similar solution of free convective flow of power law nanofluids in porous medium along a vertical cone and plate with thermal and mass convective boundary conditions. Khan and Gorla

[6] studied the effects of magnetic field on combined heat and mass transfer in non-Newtonian nanofluids over a stretching surface with prescribed wall temperature and uniform surface nanoparticle concentration. Das et al. [7] investigated the effect of buoyancy force on mixed convective Couette flow of a reactive viscous incompressible nanofluid between two concentric cylindrical pipes under bimolecular, Arrhenius and sensitised reaction rates. Chamkha et al. [8] studied the Non-Darcy natural convection flow for non-Newtonian nanofluid over a cone saturated in porous medium with uniform heat and volume fraction fluxes. Uddin et al. [9] studied the two-dimensional magnetohydrodynamic boundary layer flow of non-Newtonian power-law nanofluids past a linearly stretching sheet with a linear hydrodynamic slip boundary condition and concluded that increasing thermophoresis parameter boosts both the temperatures and nanoparticle concentration magnitudes throughout the boundary layer regime. Abbasi et al. [10] studied the peristaltic motion of a non-Newtonian nanofluid in an asymmetric channel. Bég et al. [11] studied the bio convection flow of non-Newtonian nanofluids along a horizontal flat plate in a porous medium saturated with gyrotactic microorganisms. Mahesh and Gorla [12] investigated the MHD boundary layer flow past a wedge in a non-Newtonian nanofluid. Ternik et al. [13] investigated the heat-transfer characteristics of a non-Newtonian Au nanofluid in a cubical enclosure with differentially heated side walls. Nadeem et al. [14] investigated the stagnation point flow of non-Newtonian nanofluid over an exponentially stretching surface. Hatami and Ganji [15] studied the natural convection of a non-Newtonian nanofluid flow between two vertical flat plates and concluded that Cu as nanoparticles makes larger velocity and temperature values for nanofluid compared to Ag. Ellahi et al. [16] studied the series solutions of non-Newtonian nanofluids with Reynolds' model and Vogel's model by means of the homotopy analysis method. Ternik and Rudolf [17] investigated the laminar natural convection of non-Newtonian nanofluids in a square enclosure with differentially heated side walls. Uddin et al. [18] studied the steady two-dimensional non-isothermal boundary layer flow from a heated horizontal surface which is embedded in a porous medium saturated with a non-Newtonian power-law nanofluid. Niu et al [19] concluded that increase of the slip length always results in larger flow rate of the nanofluid and the heat transfer rate of the nanofluid in the microtube can be enhanced due to the non-Newtonian rheology and slip boundary effects. Nadeem and Saleem [20] studied the rotating non-Newtonian nanofluid on a rotating cone. [Mahdy](#) and [Chamkha](#) [21] studied the heat transfer and fluid flow of a non-Newtonian nanofluid over an unsteady contracting cylinder

---

employing Buongiorno's model. Khan and Pop [22] investigated the boundary-layer flow of a nanofluid past a stretching sheet. The effect of heat source/sink is very important in cooling process industries and radiative heat transfer in which heat is transmitted from one point to another without heating the intervening medium has been found very important in the design of reliable equipment, nuclear plants, gas turbines, and various propulsion devices for aircraft, missiles, satellites, and space vehicles. Haile and Shankar [23] studied the heat and mass transfer in the boundary-layer flow of unsteady viscous nanofluid along a vertical stretching sheet in the presence of magnetic field, thermal radiation, heat generation, and chemical reaction. Zheng et al. [24] investigated the flow and radiation heat transfer of a nanofluid over a stretching sheet with velocity slip and temperature jump in porous medium. Madhu and Kishan [25] concluded that the influence of thermophoresis  $Nt$  increases the velocity, temperature, and concentration profiles for the cases of pseudoplastic, Newtonian, and dilatant fluids and the effect of Brownian motion  $Nb$  is to increase the temperature profiles and decrease the concentration profiles. Aly [26] studied the radiation and MHD boundary layer stagnation-point of nanofluid flow towards a stretching sheet embedded in a porous medium in the presence of suction/injection and heat generation/absorption with effect of the slip model and concluded that the reduced Nusselt number decreases with increase of  $Nt$  and  $Nb$ . Gangadhar [27] studied the radiation and viscous dissipation effects on chemically reacting NHD boundary layer flow of heat and mass transfer through a porous vertical flat plate. Gangadhar [28] investigated the radiation, heat generation and viscous dissipation effects on MHD boundary layer flow for the Blasius and Sakiadis flows with a convective surface boundary condition. Mohammed Ibrahim, Gangadhar and Bhaskar Reddy [29] investigated the radiation and mass transfer effects on MHD oscillatory flow in a channel filled with porous medium in the presence of chemical reaction. Sarkar et al. [30] investigated the magnetohydrodynamic peristaltic flow of nanofluids in a convectively heated vertical asymmetric channel in the presence of a transverse magnetic field and thermal radiation. Bhargava and Goyal [31] investigated the MHD non-Newtonian nanofluid flow over a permeable stretching sheet with heat generation and velocity slip. Murthy et al. [32] studied the influence of the prominent viscous dissipation and chemical reaction effects on boundary layer stagnation point flow past a stretching/shrinking sheet in a nanofluid for both assisting and opposing flows.

However, the interactions of MHD mixed convection boundary layer flow of heat and mass transfer stagnation-point flow of a non-Newtonian power-law nanofluid towards a stretching surface with thermal radiation and heat source/sink in the presence of viscous dissipation and variable suction/injection is investigated numerically. The governing boundary layer equations have been transformed to a two-point boundary value problem in similarity variables and the resultant problem is solved numerically using bvp4c MATLAB solver. The effects of various governing parameters on the fluid velocity, temperature, concentration, Skin-friction and the rate of heat and mass transfer are shown in figures and analyzed in detail.

## 2. MATHEMATICAL FORMULATION

Consider steady, laminar, heat, and mass transfer by mixed convection, boundary layer stagnation-point flow of an electrically conducting and radiating, viscous dissipative, optically dense, and non-Newtonian power-law fluid obeying the Ostwald-de Waele model (see [33]) past a heated or cooled stretching vertical surface in the presence of thermal radiation. Schematic diagram of the physical problem is shown in figure A.

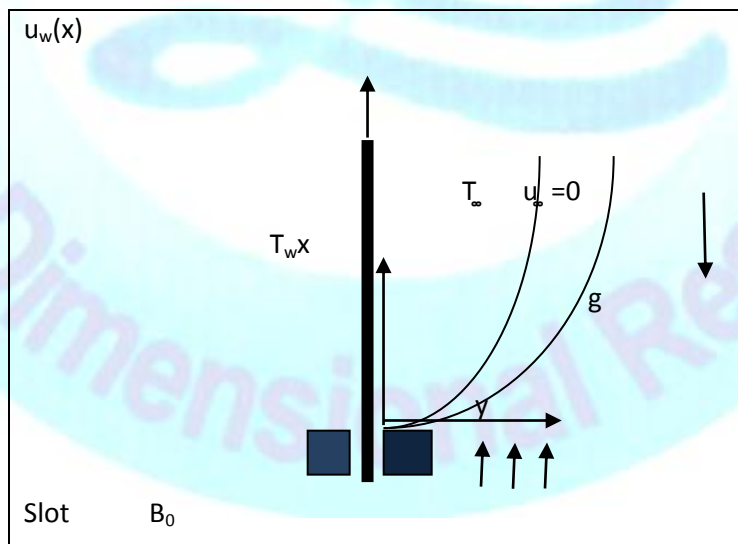


Fig.A: Schematic diagram of the physical problem.

It is assumed that the stretching velocity is given by  $u_w(x) = cx$  and the velocity distribution in frictionless potential flow in the neighborhood of the stagnation point at  $x = y = 0$  is given by  $U(x) = ax$ . We assumed that the uniform wall temperature  $T_w$  and nanoparticles volume fraction  $C_w$  are higher than those of their full stream values  $T_\infty, C_\infty$ . A uniform magnetic field is applied in the  $y$ -direction normal to the flow direction. The magnetic Reynolds number is assumed to be small so that the induced magnetic field is neglected. In addition, the Hall effect and the electric field are assumed to be negligible. The small magnetic Reynolds number assumption uncouples the Navier-Stokes equations from Maxwell's equations. All physical properties are assumed to be constant except for the density in the buoyancy force term. By invoking all of the boundary layer, Boussinesq and Rosseland diffusion approximations, the governing equations for this investigation can be written as

Continuity equation

$$\frac{\partial u}{\partial x} + \frac{\partial v}{\partial y} = 0 \quad (2.1)$$

Momentum equation

$$u \frac{\partial u}{\partial x} + v \frac{\partial u}{\partial y} = U \frac{dU}{dx} + \frac{1}{\rho} \frac{\partial \tau_{xy}}{\partial y} + g\beta(T - T_\infty) + g\beta^*(C - C_\infty) - \frac{\sigma B_0^2}{\rho} (u - U) \quad (2.2)$$

Energy equation

$$u \frac{\partial T}{\partial x} + v \frac{\partial T}{\partial y} = \alpha_m \frac{\partial^2 T}{\partial y^2} + \tau \left[ D_B \frac{\partial C}{\partial y} \frac{\partial T}{\partial y} + \frac{D_T}{T_\infty} \left( \frac{\partial T}{\partial y} \right)^2 \right] + \frac{\nu}{\rho c_p} \left( \frac{\partial u}{\partial y} \right)^2 + \frac{Q_0}{(\rho c_p)_f} (T - T_\infty) - \frac{1}{\rho c_p} \frac{\partial q_r}{\partial y} \quad (2.3)$$

$$u \frac{\partial C}{\partial x} + v \frac{\partial C}{\partial y} = D_B \frac{\partial^2 C}{\partial y^2} + \frac{D_T}{T_\infty} \frac{\partial^2 T}{\partial y^2} \quad (2.4)$$

The boundary conditions are

$$u = u_w(x) = cx, v = -v_w(x), T = T_w, C = C_w \text{ at } y = 0$$

$$u \rightarrow U(x), T \rightarrow T_\infty, C \rightarrow C_\infty \text{ as } y \rightarrow \infty \tag{2.5}$$

$u, v, T,$  and  $C$  are the  $x$  and  $y$  components of velocity, temperature, and nanoparticle volume fraction, respectively.  $g, \rho, \alpha_m, D_B, D_T, B_0, \beta$  and  $\beta^*$  are the gravitational acceleration, fluid density, thermal diffusivity, Brownian diffusion coefficient, thermophoretic diffusion coefficient, magnetic field, coefficient of thermal expansion, and coefficient of concentration of expansion, respectively.  $v_w(x) > 0$  is velocity of suction and  $v_w(x) < 0$  is velocity of injection, respectively. The term  $Q_0(T - T_\infty)$  is assumed to be the amount of heat generated or absorbed per unit volume  $Q_0$  as a coefficient constant, which may take on either positive or negative value. When the wall temperature  $T$  exceeds the free stream temperature  $T_\infty$  the source term  $Q_0 > 0$  and heat sink when  $Q_0 < 0$ . We have  $\frac{\partial u}{\partial y} > 0$  when  $\frac{a}{c} > 0$  (the ratio of free stream velocity and stretching velocity) which gives the shear stress as

$$\tau_{xy} = K \frac{\partial}{\partial y} \left( \frac{\partial u}{\partial y} \right)^n \tag{2.6}$$

where  $K$  is the consistency coefficient and  $n$  is the power-law fluid. It needs to be mentioned that, for the non-Newtonian power-law model, the case of  $n < 1$  is associated with shear thinning fluids (pseudoplastic fluids);  $n = 1$  corresponds to Newtonian fluids and  $n > 1$  applies to the case of shear thickening (dilatant).

Using the Rosseland approximation for radiation, the radiative heat flux is simplified as

$$q_r = -\frac{4\sigma^*}{3k^*} \frac{\partial T^4}{\partial y} \tag{2.7}$$

where  $\sigma^*$  and  $k^*$  are the Stefan-Boltzmann constant and the mean absorption coefficient, respectively. We assume that the temperature differences within the flow, such as the term  $T^4$ , may be expressed as a linear function of temperature. Hence, expanding  $T^4$  in a Taylor series about a free stream temperature  $T_\infty$  and neglecting higher-order terms, we get

$$T^4 = 4T_\infty^3 T - 3T_\infty^4 \quad (2.8)$$

Using (2.7) and (2.8) in the last term of (2.3), we obtain

$$\frac{\partial q_r}{\partial y} = -\frac{16\sigma^* T_\infty^3}{3k^*} \frac{\partial^2 T}{\partial y^2} \quad (2.9)$$

In order to reduce the governing equations into a system of ordinary differential equations, the following dimensionless parameters are introduced

$$\psi = \left( \frac{K/\rho}{c^{1-2n}} \right) x^{2n/(n+1)} f(\eta), \eta = y \left( \frac{c^{2-n}}{K/\rho} \right)^{1/(n+1)}, \theta = \frac{T - T_\infty}{T_w - T_\infty}, \phi = \frac{C - C_\infty}{C_w - C_\infty} \quad (2.10)$$

It is worth mentioning that the continuity equation (2.1) is identically satisfied from our choice of the stream function with  $u = \frac{\partial \psi}{\partial y}$  and  $v = -\frac{\partial \psi}{\partial x}$ .

Substituting the dimensionless parameters into (2.2)–(2.4) gives

$$n(f'')^{n-1} f''' + \left( \frac{2n}{n+1} \right) f f'' - f'^2 - M f' + M C + C^2 + \delta(\theta + N\phi) = 0 \quad (2.11)$$

$$\frac{1}{Pr} \left( 1 + \frac{4R}{3} \right) \theta'' + \left( \frac{2n}{n+1} \right) f \theta' + Nb \theta' \phi' + Nt \theta'^2 + Ec f'^2 + Q\theta = 0 \quad (2.12)$$

$$\phi'' + \left( \frac{2n}{n+1} \right) L e f \phi' + \frac{Nt}{Nb} \theta'' = 0 \quad (2.13)$$

The transformed boundary conditions can be written as

$$f(0) = \frac{2n-1}{2n} f_w, f'(0) = 1, \theta(0) = 1, \phi(0) = 1$$

$$f' \rightarrow C, \theta \rightarrow 0, \phi \rightarrow 0 \text{ as } \eta \rightarrow \infty \tag{2.14}$$

where primes denote differentiation with respect to  $\eta$

$$M = \frac{\sigma B_0^2}{\rho c}, \delta = \frac{g\beta(T_w - T_\infty)x^3 / \nu^2}{u_w^2 x^2 / \nu^2}, N = \frac{g\beta^*(C_w - C_\infty)}{g\beta(T_w - T_\infty)}$$

$$Pr = \frac{\nu}{\alpha_m} (c^2 Re_x)^{(n-1)/(n+1)}, R = \frac{4\sigma^* T_\infty^3}{kk^*}, Nb = \frac{\tau D_B (C_w - C_\infty)}{\nu} (c^2 Re_x)^{(1-n)/(n+1)}$$

$$Nt = \frac{\tau D_T (T_w - T_\infty)}{T_\infty \nu} (c^2 Re_x)^{(1-n)/(n+1)}, Le = \frac{\nu}{D_B} (c^2 Re_x)^{(n-1)/(n+1)}, Q = \frac{Q_0}{(\rho c)_f}$$

$$f_w = \left( \frac{c^{1-2n}}{K/\rho} \right)^{1/(n+1)} x^{(n-1)/(n+1)} \nu_w, Ec = \frac{u_w^2}{c_p (T_w - T_\infty)} (c^2 Re_x)^{(1-n)/(n+1)} \tag{2.15}$$

where  $Re_x = \frac{u_w x}{\nu}$  is the local Reynolds number based on the stretching velocity  $u_w(x)$  and  $k$  is the thermal conductivity.  $f_w > 0$  ( $< 0$ ) is the suction (or injection), It should be noted that  $\delta > 0$  corresponds to an assisting flow (heated plate),  $\delta < 0$  corresponds to an opposing flow (cooled plate), and  $\delta = 0$  yields forced convection flow.

The physical quantities of interest are the wall skin friction coefficient  $C_{f_x}$ , the local Nusselt number  $Nu_x$  and the local Sherwood number  $Sh_x$  which are defined as



$$\begin{aligned}
 C_{fx} &= 2[f''(0)]^n \left( \frac{(cx)^{2-n} x^n}{K/\rho} \right)^{-1/(1+n)} \\
 Nu_x &= -K \left( \frac{u_w^{2-n}}{K/\rho} \right)^{1/(n+1)} \left( 1 + \frac{4R}{3} \right) \theta'(0) \\
 Sh_x &= -D \left( \frac{u_w^{2-n}}{K/\rho} \right) \phi'(0)
 \end{aligned} \tag{2.16}$$

where  $Re_x = \frac{u_e x}{\nu_f}$  is the local Reynolds number.

### 3 SOLUTION OF THE PROBLEM

The set of equations (2.11) to (2.13) were reduced to a system of first-order differential equations and solved using a MATLAB boundary value problem solver called **bvp4c**. This program solves boundary value problems for ordinary differential equations of the form  $y' = f(x, y, p)$ ,  $a \leq x \leq b$ , by implementing a collocation method subject to general nonlinear, two-point boundary conditions  $g(y(a), y(b), p)$ . Here  $p$  is a vector of unknown parameters. Boundary value problems (BVPs) arise in most diverse forms. Just about any BVP can be formulated for solution with **bvp4c**. The first step is to write the ODEs as a system of first-order ordinary differential equations. The details of the solution method are presented in Shampine and Kierzenka [34].

### RESULTS AND DISCUSSION

The numerical results are compared in Tables 1 for local Sherwood number. Figs. 1(a)–1(c) illustrate the variation of velocity, temperature, and nanoparticles volume fraction profiles, respectively, for different values of power-law index  $n$ . The velocity, temperature, and nanoparticles volume fraction profiles decrease with the increase of power-law index  $n$  from 0.6 to 1.4. The effect of the increased values of  $n$  is to reduce the boundary layer thickness. It can be observed from Fig. 1(b) that the effect of power-law index  $n$  increases from 0.6 to 1.4; the temperature profiles decrease with an increasing viscosity of nanofluid, and thermal diffusion is depressed in the resume which cools the boundary layer and decreases the boundary layer thickness. It can also be seen from Fig. 1(c) that the increase of power-law index  $n$  from 0.6 to 1.4 decreases the nanoparticle volume fraction which decreases diffusion

of nanoparticle volume fraction (concentration) boundary layer thickness. Figs. 2-4 present the changes in the velocity, temperature and concentration profiles with the effect of magnetic parameter  $M$  for shear thinning ( $n < 1$ ), Newtonian ( $n = 1$ ), and shear-thickening ( $n > 1$ ) fluids, respectively. The velocity profiles decrease with the raising of magnetic parameter  $M$ . This is due to magnetic field opposing the transport phenomena, since the variation of magnetic parameter  $M$  causes the variation of Lorentz forces. The Lorentz force is a drag like force that produces more resistance to transport phenomena and that causes reduction in the fluid velocity. The effect of magnetic field is more in shear-thinning fluids than shear-thickening fluids. The effect of magnetic fields increases the temperature and concentration profiles (Figs. 3&4). Fig. 5-7 presents the velocity, temperature, and concentration profiles for various values of ratio of velocity parameter  $C$ . It can be observed that an increase in  $C$  causes increase in velocity profiles and significant decrease on the temperature and concentration profiles. Figs 8 – 10 show the effect of dimensionless mixed convection parameter  $\delta$  on velocity, temperature, and concentration profiles, respectively. The velocity profiles are increasing with increasing values of  $\delta$  whereas temperature and concentration profiles are decreasing with increasing values of  $\delta$ . The presence of the thermal buoyancy effects represented by finite values of the mixed parameter has the tendency to induce more flow along the surface at the expense of small reductions in the temperature and concentration. Distinctive peaks in the velocity profiles which are characteristics of free convection flows are also observed as  $\delta$  increases.

Fig. 11-13 shows the effect of thermal buoyancy ratio  $N$  on velocity, temperature and concentration profiles for shear-thinning ( $n < 1$ ), Newtonian ( $n = 1$ ), and shear-thickening ( $n > 1$ ) fluids, respectively. It is noticed that the increase of  $N$  values has a tendency to increase the buoyancy effects changing more induced flow along the stretching sheet in the vertical direction reflected by the increase in the fluid velocity and decrease in the fluid temperature and concentration. This enhancement in the fluid velocity has more in shear-thinning fluid ( $n < 1$ ) than shear-thickening fluid ( $n > 1$ ). This reduction in the fluid temperature and concentration has more in shear-thinning fluid ( $n < 1$ ) than shear-thickening fluid ( $n > 1$ ). Figs. 14-16 present the velocity, temperature, and concentration profiles for various values of ratio of suction/injection parameter  $f_w$ . It can be observed that an increase in  $f_w$  focuses decrease on the velocity, temperature and concentration profiles.

The effect of thermophoresis parameter  $Nt$  is to increase velocity, temperature, and concentration profiles for both Newtonian and non-Newtonian fluids are noticed in Fig. 17-19. It is observed that velocity, temperature and concentration of the fluid increases with increases the values of  $Nt$ . Fig. 20-22 exhibit dimensionless velocity, temperature and concentration profiles for various values of Brownian motion parameter  $Nb$ . It can be seen that the velocity and temperature profile slightly increases with an increase in the value of Brownian motion parameter  $Nb$ . The concentration profiles decrease with the value of Brownian motion parameter  $Nb$ . The variations in heat source/sink parameter  $Q$  on velocity, temperature and concentration profiles are given in Fig. 23-25; from the figure it can be seen that the velocity as well as temperature profiles increases with the increase of heat source/sink parameter  $Q$  but concentration increases near the plate and decreases for away the plate. A gradually increasing heat source/sink parameter increases the thermal boundary layer thickness which physically reveals the fact that an increase in the heat source/sink parameter means an increase in the heat generated inside the boundary layer which leads to higher temperature field. It is noted that the temperature profiles decrease for increasing strength of heat sink and due to increase of heat source strength the temperature increases. So the thickness of the thermal boundary layer reduces for increase with heat source parameter. These results are very much significant for the flow where heat transfer is given prime importance. Figs. 26-27 are drawn for the velocity and temperature profiles for different values of Prandtl number  $Pr$  for the cases shear-thinning ( $n < 1$ ), Newtonian ( $n = 1$ ), and shear-thickening ( $n > 1$ ) fluids. The effect of Prandtl number  $Pr$  is to reduce the velocity and temperature profiles for both Newtonian and non-Newtonian fluids. Physically, fluids with smaller Prandtl number  $Pr$  have larger thermal diffusivity. Fig. 28 shows the effect of radiation parameter  $R$  on the velocity profiles for both Newtonian and non-Newtonian fluids. It is noticed from the figure that the velocity of the fluid increases with the increase of radiation parameter  $R$  values. It can be shown from Fig. 29 that temperature of the fluid increases with the increase of radiation parameter  $R$ . As expected, an increase of the radiation parameter  $R$  has the tendency to increase the effect of conduction as well as increasing the temperature at each point away from the surface. Hence, higher values of radiation parameter  $R$  imply a higher surface heat flux. The variations in Eckert number  $Ec$  on velocity and temperature profiles are given in Fig. 30-31; from the figure it can be seen that the velocity decreases but temperature increases with the increase of Eckert number  $Ec$  values.

Fig. 32 shows the effect of  $Nt$ ,  $Nb$  and  $f_w$  on local Nusselt number for shear-thinning ( $n < 1$ ), Newtonian ( $n = 1$ ), and shear-thickening ( $n > 1$ ) fluids, respectively. It is noticed that the increase of  $Nt$  or  $Nb$  values has a tendency to decrease the Nusselt number whereas increase the Nusselt number with an increase the values of  $f_w$ .

#### 4 CONCLUSIONS

In this paper two-dimensional MHD mixed convection boundary layer flow of heat and mass transfer stagnation-point flow of a non-Newtonian power-law nanofluid towards a stretching surface with thermal radiation and heat source/sink in the presence of viscous dissipation and variable suction/injection is investigated numerically. Using similarity transformations, the governing equations are transformed to self-similar ordinary differential equations which are then solved using Bvp4c MATLAB solver. From the study, the following remarks can be summarized.

1. Fluid velocity, temperature and concentration increases with an increasing the values of thermophoresis parameter.
2. Fluid velocity, temperature and concentration decreases with an increasing the values of suction/injection parameter.
3. Fluid velocity decreases and fluid temperature increases with the influence of viscous dissipation.
4. Fluid velocity and temperature of the fluid increases with a rising the values of Brownian motion parameter whereas concentration decreases with the influence of Brownian motion parameter.
5. Local Nusselt number decreases with an increase Brownian motion parameter and thermophoresis parameter but in the presence of suction/injection the local Nusselt number increases.

**Table 1:** Comparison of  $-\phi'(0)$  when  $Pr=Le=10, n=1, M = fw = Ec = \delta = Q = 0$ .

Nt	Nb	$f''(0)$			
		Aly [26]	Zheng et al. [24]	KhanandPop[22]	Present study
0.1	0.1	2.12938	2.12939	2.1294	2.129384
0.2	0.1	2.27401	2.27402	2.2740	2.273994
0.3	0.1	2.52868	2.52863	2.5286	2.528576
0.4	0.1	2.79519	2.79517	2.7952	2.795036
0.5	0.1	3.03510	3.03514	3.0351	3.034861
0.1	0.2	2.38182	2.38187	2.3819	2.381863
0.1	0.3	2.40995	2.41001	2.4100	2.410012
0.1	0.4	2.39961	2.39965	2.3997	2.399644
0.1	0.5	2.38256	2.38257	2.3836	2.383565

## REFERENCES

- Schowalter, W. R., (2004), "The application of boundary-layer theory to power-law pseudoplastic fluids: similar solutions," *AICHE Journal*, Vol. 6, No. 1, pp. 24–28.
- Hatami, M., Hatami, J., Ganji, D.D., (2013), Computer simulation of MHD blood conveying gold nanoparticles as a third grade non-Newtonian nanofluid in a hollow porous vessel, *computer Methods and Programs in Biomedicine*, Vol.113, pp.632-641.
- Rashad, A. M., EL-Hakim, M. A., Abdou, M. M. M., (2011), Natural convection boundary layer of a non-Newtonian fluid about a permeable vertical cone embedded in a porous medium saturated with a nanofluid, *Computers & Mathematics with Applications*, Vol. 62, Pp. 3140-3151.
- KeshavarzMoraveji M., A.R. Beheshti, A.R., (2014), CFD Study of the Turbulent Forced Convective Heat Transfer of Non-Newtonian Nanofluid, *Iranian Journal of Chemical Engineering*, Vol. 11, No. 2.

5. Khan, W.A., JashimUddin, M., Ismail A.I.M., (2015), Non-similar solution of free convective flow of power law nanofluids in porous medium along a vertical cone and plate with thermal and mass convective boundary conditions, Canadian Journal of Physics, Vol. 93, No. 10, pp. 1144-1155.
6. Waqar A. Khan and Rama Subba Reddy Gorla (2012), Effect of Magnetic Field on Heat Transfer in Non-Newtonian Nanofluids Over a Nonisothermal Stretching Wall, J. Heat Transfer, Vol. 134, No.10.
7. Das, S.; Chakraborty, S.; Jana, R. N.; Makinde, O. D. (2015), Mixed Convective Couette Flow of Reactive Nanofluids Between Concentric Vertical Cylindrical Pipes, [Journal of Nanofluids](#), Vol. 4, No 4, pp. 485-493(9).
8. Chamkha.A., Abbasbandy.S., Rashad.A.M., (2015), Non-Darcy natural convection flow for non-Newtonian nanofluid over a cone saturated in porous medium with uniform heat and volume fraction fluxes, International journal of Numerical Methods for Heat and Fluid Flow, Vol.25, No.2, pp.422-437.
9. Uddin, M. J., Ferdows, M., Anwar Be'g, O., (2014), Group analysis and numerical computation of magneto-convective non-Newtonian nanofluid slip flow from a permeable stretching sheet, [ApplNanosci.](#), Vol.4, pp.897–910.
10. FahadMunirAbbasi, Tasawar Hayat, Bashir Ahmad, and Guo-Qian Chen, (2014), Peristaltic Motion of a non-Newtonian Nanofluid in an Asymmetric Channel, Z. Naturforsch., Vol. 69a, pp.451 – 461.
11. Anwar Bég, O., JashimUddin, MD., and KhanW. A., (2015), Bioconvective non-newtoniannanofluid transport in porous media containing micro-organisms in a moving free stream, Journal of Mechanics in Medicine and Biology, Vol. 15, No. 05.
12. Kumari, Mahesh; Gorla, Rama Subba Reddy, (2015), MHD Boundary Layer Flow of a Non-Newtonian Nanofluid Past a Wedge, [Journal of Nanofluids](#), Vol. 4, No. 1, pp. 73-81(9).
13. Primo` Ternik, RebekaRudolf, Zoran Zuni, (2015), Heat-transfer characteristics of a non-Newtonian Au nanofluid in a cubical enclosure with differentially heated side walls, [Materiali in tehnologije / Materials and technology](#), Vol. 49, No.1, pp.87–93.

14. Nadeem S., Sadiq M. A, Jung-il Choi, Changhoon Lee, (2014), Exponentially Stagnation Point Flow of Non-Newtonian Nanofluid over an Exponentially Stretching Surface, International Journal of Nonlinear Sciences and Numerical Simulation. Vol. 15, Issue 3-4, Pp.171–180.
15. Hatami M., Ganji D.D., (2014), Natural convection of sodium alginate (SA) non-Newtonian nanofluid flow between two vertical flat plates by analytical and numerical methods, Case Studies in Thermal Engineering, Vol.2, pp.14–22.
16. Ellahi R., Raza M., Vafai K., (2012), Series solutions of non-Newtonian nanofluids with Reynolds' model and Vogel's model by means of the homotopy analysis method, Mathematical and Computer Modelling, Vol.55, pp.1876–1891.
17. Ternik. P, and Rudolf R., (2013), Laminar natural convection of Non Newtonian nanofluids in a square enclosure with differentially heated side walls, Int J Simul Model, Vol.12, pp.5-16.
18. MdJashimUddin, N H MdYusoff, O Anwar Bégand Ahamd Izani Ismail, (2013), Lie group analysis and numerical solutions for non-Newtonian nanofluid flow in a porous medium with internal heat generation, The Royal Swedish Academy of Sciences, Physica Scripta, Vol. 87, No.2.
19. Jun Niu, Ceji Fu, Wenchang Tan (2012), Slip-Flow and Heat Transfer of a Non-Newtonian Nanofluid in a Microtube, PLoS ONE, Vol. 7, pp.1-9.
20. Nadeem, S., and Saleem, S., (2014), Analytical Study of Rotating Non-Newtonian Nanofluid on a Rotating Cone, Journal of Thermophysics and Heat Transfer, Vol. 28, No. 2, pp. 295-302.
21. [Mahdy A.](#), [Chamkha A.](#), (2015), Heat transfer and fluid flow of a non-Newtonian nanofluid over an unsteady contracting cylinder employing Buongiorno's model, International Journal of Numerical Methods for Heat & Fluid Flow, Vol. 25, Iss: 4, pp.703 – 723.
22. Khan W. A. and Pop, I., (2010), Boundary-layer flow of a nanofluid past a stretching sheet," International Journal of Heat and Mass Transfer, Vol. 53, No. 11-12, pp. 2477–2483.
23. Eshetu Haile and B. Shankar, (2014), Heat and Mass Transfer in the Boundary Layer of Unsteady Viscous Nanofluid along a Vertical Stretching Sheet, Hindawi Publishing Corporation, Journal of Computational Engineering, Vol. 2014, pp.1-17.
24. Zheng, L., Zhang, C., Zhang, X., and Zhang, J., (2013), Flow and radiation heat transfer of a nanofluid over a stretching sheet with velocity slip and temperature jump in porous medium,

Journal of the Franklin Institute. Engineering and Applied Mathematics, Vol. 350, No. 5, pp. 990–1007.

25. MachaMadhu and NaikotiKishan, (2015), Magnetohydrodynamic Mixed Convection Stagnation-Point Flow of a Power-Law Non-Newtonian Nanofluid towards a Stretching Surface with Radiation and Heat Source/Sink, Hindawi Publishing Corporation, Journal of Fluids, Vol. 2015, pp.1-14.
26. Emad H. Aly (2015), Radiation and MHD Boundary Layer Stagnation-Point of Nanofluid Flow towards a Stretching Sheet Embedded in a Porous Medium: Analysis of Suction/Injection and Heat Generation/Absorption with Effect of the Slip Model, Hindawi Publishing Corporation, Mathematical Problems in Engineering, Vol.2015, pp.1-20.
27. Gangadhar, K., (2012), Radiation and viscous dissipation effects on chemically reacting NHD boundary layer flow of heat and mass transfer through a porous vertical flat plate, Journal of Energy, Heat and Mass Transfer, Vol.34, pp.245-259.
28. Gangadhar, K., (2015), Radiation, Heat generation and viscous dissipation effects on MHD Boundary layer flow for the Blasius and Sakiadis flows with a convective surface boundary condition, Journal of Applied Fluid Mechanics, Vol. 8, No. 3, pp. 559-570.
29. Mohammed Ibrahim, S., Gangadhar K., and Bhaskar Reddy, N., (2015), Radiation and mass transfer effects on mhd oscillatory flow in a channel filled with porous medium in the presence of chemical reaction, Journal of Applied Fluid Mechanics, Vol. 8, No. 3, pp. 529- 537.
30. Sarkar, B. C.; Das, S.; Jana, R. N.; Makinde, O. D. (2015), Magnetohydrodynamic Peristaltic Flow of Nanofluids in a Convectively Heated Vertical Asymmetric Channel in Presence of Thermal Radiation, Journal of Nanofluids, Vol. 4, No. 4, pp. 461-473(13).
31. Rama Bhargava, Mania Goyal, (2014), MHD Non-Newtonian Nanofluid Flow over a Permeable Stretching Sheet with Heat Generation and Velocity Slip, International Scholarly and Scientific Research & Innovation, Vol:8, No:6, pp.910-916.
32. Murthy, P. V. S. N.; RamReddy, Ch.; Chamkha, A. J.; Rashad, A. M., (2015), Significance of Viscous Dissipation and Chemical Reaction on Convective Transport in a Boundary Layer Stagnation Point Flow Past a Stretching/Shrinking Sheet in a Nanofluid, Journal of Nanofluids, Vol. 4, No.2, pp. 214-222(9).



33. Metzner, A. B., (1965), "Heat transfer in non-Newtonian fluid," Advances in Heat Transfer, Vol. 2, pp. 357–397.
34. Shampine, L. F., and Kierzenka, J., (2000), "Solving boundary value problems for ordinary differential equations in MATLAB with bvp4c," Tutorial Notes.

